Indomethacin-Containing Nanoparticles Derived from Amphiphilic Polynorbornene: A Model ROMP-Based Drug Encapsulation System

Paul A. Bertin, Keith J. Watson, and SonBinh T. Nguyen*

Department of Chemistry and Center for Nanofabrication and Molecular Self-Assembly, Northwestern University, Evanston, Illinois 60208-3113

Received November 20, 2003; Revised Manuscript Received May 14, 2004

ABSTRACT: A series of monodisperse amphiphilic diblock copolymers containing a high-density of covalently linked indomethacin as the hydrophobic block and pendant hexaethylene glycol monomethyl ether as the hydrophilic block have been synthesized from ring-opening metathesis polymerization (ROMP) using $Cl_2(PCy_3)_2Ru{=}CHPh$. Dynamic light scattering (DLS), transmission electron microscopy (TEM), and ^1H NMR spectroscopy have been used to investigate the directed-assembly of these polynorbornene-based copolymers into polymeric nanoparticles in aqueous media as a function of copolymer composition, concentration, and degree of polymerization. The block copolymers formed micelle-like aggregates in the aqueous phase with mean diameters ranging from 993 ± 270 nm to 94 ± 14 nm by TEM. In general, the aggregate size decreased as the overall copolymer length decreased. After incubation in an acidic environment (pH = 3) at 37 °C for 48 h, 20% of the indomethacin was released from the nanoparticles.

Introduction

The formation of core−shell polymeric nanoparticles through the association of amphiphilic macromolecules has been an intense field of research over the last few decades. It is well known that, in the presence of a solvent or solvent mixture that is selective for one block, amphiphilic block copolymers have the ability to assemble into colloidal aggregates of various morphologies.[1] In particular, significant interest has been focused on the formation of polymeric micelles and nanoparticles from amphiphilic block copolymers in aqueous media.[2−4] This organized association occurs as polymer chains reorganize to minimize interactions between the insoluble hydrophobic blocks and water. The resulting nanoparticles presumably possess cores composed of hydrophobic block segments surrounded by outer shells of hydrophilic block segments. Numerous realized or potential technological applications for the solubilization of various hydrophobic materials are based on this structural property. For example, the core−shell structures of amphiphilic micellar assemblies have been utilized as novel carrier systems in the field of drug delivery.[5−7] The use of these systems is motivated predominantly by the problematic properties of some low-molecular-weight drug candidates, such as side effects and toxicity associated with poor specificity, poor water solubility, low bioavailability, as well as rapid elimination.[8]

The concept of micelle-forming block copolymer−drug conjugates was introduced by Pratten et al.[9] in which one block is conjugated with hydrophobic drug molecules and the other block remains unmodified and water-soluble. The resulting copolymer−drug conjugates were found to form micelles with a core comprised of drug-modified segments protected by a shell comprised of poly(ethylene oxide) (PEO) in an aqueous environment. More recently, significant advancements to this approach have been reported for the preparation of polymeric micelles exhibiting antitumor activity.[10−12] The enhanced permeability and retention (EPR effect)[13] of solid tumors toward macromolecules have made them attractive targets for such nanoparticle drug carriers. In addition, the proliferation of some solid tumors under hypoxic conditions results in acidic extracellular environments,[14] suggesting that drug release rates from the nanoparticles can be controlled by the choice of linker.

The aim of this study was to prepare polynorbornene-based nanoparticles from amphiphilic drug-containing block copolymers and to evaluate their potential application as novel drug delivery vehicles. With the advent of well-defined, functional-group-tolerant metal alkylidene initiators such as $Cl_2(PCy_3)_2Ru{=}CHPh$,[15,16] ring-opening metathesis polymerization (ROMP) has emerged as an attractive approach for the preparation of synthetic polymers with biological activity.[17] Recently, we demonstrated that norbornene-modified antitumor drugs are amenable to the synthesis of well-defined drug-containing polymers via ROMP.[18] Herein, we describe the synthesis and micelle-like aggregation of a series of monodisperse ROMP-based amphiphilic block copolymers composed of hydrophobic indomethacin-containing monomers and hydrophilic hexa(ethylene oxide)-containing monomers. The copolymers were characterized by GPC, ^1H NMR, and ^{13}C NMR spectroscopy. The aggregation of these AB-type copolymers into core−shell nanoparticles in aqueous media provides an approach for protecting a high-density of drug molecules from premature degradation with a dense palisade of tethered ethylene oxide segments known to produce a stealth effect for in vivo applications.[19] Physicochemical properties of the micelle-like aggregates were characterized by transmission electron microscopy, dynamic light scattering, and ^1H NMR spectroscopy. In addition, the release behavior of indomethacin from the copolymeric nanoparticles in acidic media was investigated.

Experimental Section

General Considerations and Materials. All manipulations were performed under a dry nitrogen atmosphere using either standard Schlenk techniques or an inert-atmosphere glovebox, unless otherwise noted. Methylene chloride was

* To whom correspondence should be addressed. E-mail: stn@northwestern.edu.

10.1021/ma035741+ CCC: $27.50
Published on Web 09/30/2004

dried over calcium hydride. THF was dried over Na/benzophenone. All solvents were distilled under nitrogen and saturated with nitrogen prior to use. Dimethyl sulfoxide (DMSO) (99.9%, HPLC grade) was purchased from Aldrich and used as received. Catalyst $Ru(PCy_3)_2$=CHPh was purchased from Strem Chemicals and used as received. Deuterated solvents were purchased from Cambridge Isotope Laboratories and used without further purification, except for $CDCl_3$, which was distilled over calcium hydride and vacuum transferred into an airtight solvent bulb followed by transfer to an inert-atmosphere glovebox. Spectra/Por RC (MWCO = 3500) dialysis membranes were purchased from Spectrum Laboratories. Formvar/Carbon, 400-mesh copper TEM grids were purchased from Ted Pella, Inc. Indomethacin was purchased from Sigma, and hexaethylene glycol monomethyl ether was purchased from TCI America. All other reagents were purchased from Aldrich and used without further purification. α-Bromo-α′-(*exo*-5-norbornene-2-ol)-*p*-xlyene[20] and [1-(4-chloro-benzoyl)-5-methoxy-2-methyl-1*H*-indol-3-yl]-acetic acid 2,5-dioxo-pyrrolidin-1-yl ester (indomethacin−NHS)[21] were prepared following literature procedures. All flash chromatography was carried out using a 56-mm inner-diameter column containing 200-mm length of silica gel under a positive pressure of lab air.

Instrumentation. ^{1}H and ^{13}C NMR spectra were recorded on a Varian INOVA 500 FT-NMR spectrometer (499.6 MHz for ^{1}H NMR, 125.6 MHz for ^{13}C NMR). ^{1}H NMR data are reported as follows: chemical shift {multiplicity (b = broad, s = singlet, d = doublet, t = triplet, q = quartet, qn = quintet, and m = multiplet), integration, and peak assignments}. ^{1}H and ^{13}C chemical shifts are reported in ppm downfield from tetramethylsilane (TMS). High-resolution electron-impact mass spectrometric data (HREIMS) were obtained on a VG 70SE instrument. Elemental analyses were provided by Atlantic Microlab, Inc. (Norcoss, GA). Polymer molecular weights were measured on a Waters gel-permeation chromatograph (GPC) equipped with Breeze software, a 717 autosampler, Shodex KF-803L and Shodex KF-806L GPC columns in series with a Shodex KF-G guard column; THF was used as the eluent at a flow rate of 1.0 mL per min, and the instrument was calibrated with 15 polystyrene standards from Aldrich (M_n = 760−1 880 000 Da).

Synthesis of 2-{[4-(Bicyclo[2.2.1]hept-5-en-2-*exo*-yloxy)-methyl]benzyl}-1*H*-isoindole-1,3(2*H*)-dione (2). Into a 50-mL Schlenk flask were added potassium phthalimide (696 mg, 3.76 mmol) and α-bromo-α′-(*exo*-5-norbornene-2-ol)-*p*-xlyene (1.00 g, 3.41 mmol). The flask was placed under nitrogen, degassed DMF (20 mL) was added, and the mixture was heated at 100 °C for 12 h. Upon cooling to room temperature, the mixture was transferred to a 500-mL separatory funnel and diluted with ethyl acetate (200 mL). The mixture was washed with 10% aqueous sodium bicarbonate (2 × 100 mL), 10% sodium citrate (100 mL), and brine (2 × 100 mL). The organic layer was dried over Na_2SO_4 and filtered. The solvent was removed on the rotary evaporator. The residue was purified by flash chromatography (30% EtOAc/hexanes) to give a white solid (1.15 g, 3.20 mmol, 94%). ^{1}H NMR ($CDCl_3$): δ 1.39−1.72 (m, 4H, 3- and 7-norbornenyl-H_2), 2.79 (b, 1H, 1-norbornenyl-*H*), 2.91 (b, 1H, 4-norbornenyl-*H*), 3.55 (m, 1H, 2-norbornenyl-*H*), 4.49 (m, 2H, CH_2−O), 4.83 (b, 2H, CH_2−N), 5.89 (m, 1H, 6-norbornenyl-*H*), 6.16 (m, 1H, 5-norbornenyl-*H*), 7.30 (m, 2H, aromatic-*H*), 7.41 (m, 2H, aromatic-*H*), 7.70 (m, 2H, aromatic-*H*), 7.83 (m, 2H, aromatic-*H*). ^{13}C NMR ($CDCl_3$): δ 34.6 (3-norbornenyl-*C*), 40.6 (*C*H_2−N), 41.5 (4-norbornenyl-*C*), 46.2 (7-norbornenyl-*C*), 46.6 (1-norbornenyl-*C*), 71.0 (O−*C*H_2−Ph), 80.2 (2-norbornenyl-*C*), 123.5 (aromatic-*C*), 128.1 (aromatic-*C*), 128.9 (aromatic-*C*), 132.3 (aromatic-*C*), 133.3 (6-norbornenyl-*C*), 134.2 (aromatic-*C*), 135.7 (aromatic-*C*), 138.8 (aromatic-*C*), 140.9 (5-norbornenyl-*C*), 168.2 (*C*O−NCH$_2$). HREIMS: calcd for $C_{23}H_{21}NO_3$, 359.1521; found, 359.1523.

Synthesis of 4-[(Bicyclo[2.2.1.]hept-5-en-2-*exo*-yloxy)-methyl]benzylamine (3). Into a 50-mL Schlenk flask was added **2** (1.00 g, 2.78 mmol). The flask was placed under nitrogen, and degassed ethanol (25 mL) was added via cannula, followed by the injection of hydrazine hydrate (0.40 mL). The flask was capped with a reflux condenser connected to a nitrogen bubbler, and the reaction mixture was heated at 80 °C for 12 h. Upon cooling to room temperature, the mixture was poured into water (200 mL) and extracted with ether (3 × 100 mL). The organic fragments were dried over Na_2SO_4 and filtered. The solvent from the filtrate was removed on the rotary evaporator, yielding the desired product as a colorless oil (638 mg, 2.53 mmol, 91%). ^{1}H NMR ($CDCl_3$): δ 1.40−1.75 (m, 4H, 3- and 7-norbornenyl-H_2), 1.89 (b, 2H, NH_2), 2.81 (b, 1H, 1-norbornenyl-*H*), 2.94 (b, 1H, 4-norbornenyl-*H*), 3.58 (m, 1H, 2-norbornenyl-*H*), 3.85 (b, 2H, CH_2−N), 4.50 (m, 2H, CH_2−O), 5.91 (m, 1H, 6-norbornenyl-*H*), 6.17 (m, 1H, 5-norbornenyl-*H*), 7.29 (m, 4H, aromatic-*H*). ^{13}C NMR ($CDCl_3$): δ 34.7 (3-norbornenyl-*C*), 40.6 (4-norbornenyl-*C*), 46.2 (7-norbornenyl-*C*), 46.3 (*C*H_2−NH$_2$), 46.6 (1-norbornenyl-*C*), 71.1 (O−*C*H_2−Ph), 80.2 (2-norbornenyl-*C*), 127.4 (aromatic-*C*), 128.1 (aromatic-*C*), 133.3 (6-norbornenyl-*C*), 137.7 (aromatic-*C*), 140.9 (5-norbornenyl-*C*), 142.3 (aromatic-*C*). HREIMS: calcd for $C_{15}H_{19}NO$, 229.1467; found, 229.1466.

Synthesis of *N*-[4-(Bicyclo[2.2.1]hept-5-en-2-*exo*-yloxymethyl)-benzyl]-2-[1-(4-chlorobenzoyl)-5-methoxy-2-methyl-1*H*-indol-3-yl]-acetamide (4). Into a 50-mL Schlenk flask were added **3** (400 mg, 1.74 mmol) and indomethacin−NHS (800 mg, 1.76 mmol). The flask was placed under nitrogen, and degassed DMF (30 mL) was added via cannula. The mixture was stirred for 12 h at room temperature and transferred to a 500-mL separatory funnel with ethyl acetate (200 mL). The mixture was washed with 10% aqueous sodium bicarbonate (2 × 100 mL), 10% aqueous sodium citrate (100 mL), and saturated brine (2 × 100 mL). The organic layer was collected and dried over Na_2SO_4 and filtered. The solvent was removed on the rotary evaporator, and the residue was purified by flash chromatography (10% EtOAc/CH_2Cl_2) to give a light yellow solid (962 mg, 1.69 mmol, 97%). ^{1}H NMR ($CDCl_3$): δ 1.40−1.75 (m, 4H, 3- and 7-norbornenyl-H_2), 2.37 (b, 3H, indole-CH_3), 2.81 (b, 1H, 1-norbornenyl-*H*), 2.94 (b, 1H, 4-norbornenyl-*H*), 3.58 (m, 1H, 2-norbornenyl-*H*), 3.70 (s, 2H, NHC=OCH_2), 3.79 (s, 3H, OCH_3), 4.40 (d, 2H, CH_2NH), 4.48 (m, 2H, OCH_2), 5.88 (b, 1H, N*H*), 5.91 (m, 1H, 6-norbornenyl-*H*), 6.17 (m, 1H, 5-norbornenyl-*H*), 6.69 (m, 1H, aromatic-*H*), 6.86 (m, 2H, aromatic-*H*), 7.12 (m, 2H, aromatic-*H*), 7.24 (m, 2H, aromatic-*H*), 7.47 (m, 2H, aromatic-*H*), 7.63 (m, 2H, aromatic-*H*). ^{13}C NMR ($CDCl_3$): δ 13.5 (*C*H_3-indole), 32.4 (NHCO*C*H_2), 34.7 (3-norbornenyl-*C*), 40.6 (4-norbornenyl-*C*), 43.5 (Ph*C*H_2NH), 46.2 (7-norbornenyl-*C*), 46.6 (1-norbornenyl-*C*), 55.9 (O−*C*H_3), 70.9 (O−*C*H_2−Ph), 80.3 (2-norbornenyl-*C*), 100.8 (indole-*C*), 112.7 (indole-*C*), 112.9 (indole-*C*), 115.4 (indole-*C*), 127.7 (indole-*C*), 128.1 (aromatic-*C*), 129.4 (aromatic-*C*), 130.4 (aromatic-*C*), 131.0 (aromatic-*C*), 131.3 (aromatic-*C*), 133.3 (6-norbornenyl-*C*), 133.7 (indole-*C*), 136.5 (indole-*C*), 137.4 (aromatic-*C*), 138.4 (aromatic-*C*), 139.7 (aromatic-*C*), 140.9 (5-norbornenyl-*C*), 156.5 (indole-*C*), 168.4 (indole-*C*O), 170.0 (NH−*C*O−CH$_2$). HREIMS: calcd for $C_{34}H_{33}ClN_2O_4$, 568.2129; found, 568.2129. Anal. Calcd for $C_{34}H_{33}ClN_2O_4$: C, 71.76; H, 5.84; N, 4.92; Cl, 6.23. Found: C, 71.53; H, 5.84; N, 4.82; Cl, 6.33.

Synthesis of 5-(4-{2-*exo*-[2-(2-{2-[2-(2-Methoxy-ethoxy)-ethoxy]-ethoxy}-ethoxy)-ethoxy]-ethoxymethyl}benzyloxy)-bicyclo[2.2.1]hept-2-ene (5). Dried and oil-free Na metal spheres (58.6 mg, 2.56 mmol) were added to hexaethylene glycol monomethyl ether (506 mg, 1.71 mmol) in a 50-mL Schlenk flask. The flask was placed under nitrogen, and THF (10 mL) was added via cannula. The flask was capped with a reflux condenser connected to a nitrogen bubbler, and the reaction mixture was heated at 70 °C for 12 h and then cooled to room temperature. In a separate 50-mL Schlenk flask, α-bromo-α′-(*exo*-5-norbornene-2-ol)-*p*-xlyene (500 mg, 1.71 mmol) was added and placed under nitrogen followed by the addition of THF (10 mL). To this flask was added the Na alkoxide solution via cannula, and the mixture was refluxed at 70 °C for an additional 12 h. Upon cooling to room temperature, the mixture was concentrated, poured into CH_2Cl_2 (100 mL), and filtered to remove NaBr. The solvent was removed on the rotary evaporator, and the remaining residue was purified by flash chromatography (5% MeOH/CH_2Cl_2) to

Table 1. Properties of Copolymers from 4 and 5

entry	copolymer	yield (%)	M_n[a]	PDI[a]	$\mathbf{4}/\mathbf{5}_{NMR}$	$\mathbf{4}/\mathbf{5}_{theor}$[b]	trans/cis
1	$\mathbf{4}_{89}$-*b*-$\mathbf{5}_{11}$	93	37 900	1.34	8.1	8.1	2.8
2	$\mathbf{4}_{75}$-*b*-$\mathbf{5}_{25}$	94	35 800	1.16	3.2	3.0	2.5
3	$\mathbf{4}_{50}$-*b*-$\mathbf{5}_{50}$	91	34 700	1.30	1.2	1.0	2.4
4	$\mathbf{4}_{35}$-*b*-$\mathbf{5}_{35}$	92	31 500	1.08	1.2	1.0	2.1
5	$\mathbf{4}_{35}$-*b*-$\mathbf{5}_{15}$	96	23 400	1.22	2.6	2.3	2.4
6	$\mathbf{4}_{35}$-*b*-$\mathbf{5}_{7}$	94	19 600	1.16	5.6	5.0	2.0

[a] Estimated by GPC with linear polystyrene standards. [b] Calculated on the basis of the reaction stoichiometry.

give a clear oil (825 mg, 1.62 mmol, 95%). ^{1}H NMR ($CDCl_3$): δ 1.41−1.77 (m, 4H, 3- and 7-norbornenyl-H_2), 2.82 (b, 1H, 1-norbornenyl-*H*), 2.94 (b, 1H, 4-norbornenyl-*H*), 3.38 (s, 3H, OCH_3), 3.53−3.70 (m, 24H, OCH_2CH_2O), 4.51−4.55 (m, 5H, $CH_2-C_6H_4-CH_2$ and 2-norbornenyl-*H*), 5.91 (m, 1H, 6-norbornenyl-*H*), 6.19 (m, 1H, 5-norbornenyl-*H*), 7.32 (b, 4H, aromatic-*H*). ^{13}C NMR ($CDCl_3$): δ 34.6 (3-norbornenyl-*C*), 40.6 (4-norbornenyl-*C*), 46.2 (7-norbornenyl-*C*), 46.6 (1-norbornenyl-*C*), 59.2 (O−*C*H$_3$), 69.5−71.1 (m, O*C*H$_2$−*C*H$_2$O), 72.1 (O−*C*H$_2$−Ph), 73.2 (Ph−*C*H$_2$−O), 80.1 (2-norbornenyl-*C*), 127.8 (aromatic-*C*), 128.0 (aromatic-*C*), 133.3 (6-norbornenyl-*C*), 137.6 (aromatic-*C*), 138.5 (aromatic-*C*), 140.9 (5-norbornenyl-*C*). HREIMS: calcd for $C_{28}H_{44}O_8$, 508.3036; found, 508.3034. Anal. Calcd for $C_{28}H_{44}O_8$: C, 66.12; H, 8.72. Found: C, 66.28; H, 8.79.

General Procedure for the Synthesis of $\mathbf{4}_m$-*b*-$\mathbf{5}_n$ Block Copolymers. Control over copolymer chain length and block composition was achieved by varying monomer-to-catalyst ratios. An example procedure is presented for the synthesis of $\mathbf{4}_{35}$-*b*-$\mathbf{5}_{15}$. In an inert atmosphere glovebox, monomer **4** (100.0 mg, 0.176 mmol) was weighed into a 20-mL scintillation vial equipped with a magnetic stirring bar. Dry CH_2Cl_2 (3 mL) was added, followed by a solution of catalyst **6** (4.1 mg, 0.0050 mmol) in dry CH_2Cl_2 (1.0 mL). The mixture was stirred for 30 min at room temperature. After 30 min, a solution of monomer **5** (38.3 mg, 0.075 mmol) in dry CH_2Cl_2 (1.0 mL) was added and stirred for an additional 30 min. The polymerization was terminated with the addition of ethyl vinyl ether (0.5 mL). The copolymer $\mathbf{4}_{35}$-*b*-$\mathbf{5}_{15}$ (120 mg, 96%) was isolated by pouring the mixture into an Erlenmeyer flask containing rapidly stirred hexanes (150 mL), filtering, and repeatedly washing the off-white precipitate with fresh hexanes (4 × 50 mL). GPC (THF): M_n = 23 400; PDI = 1.22. ^{1}H NMR ($CDCl_3$): see Figure 2, δ 1.10−1.26 (bm), 1.58 (bm), 1.92 (bm), 2.32 (bs), 2.57−2.68 (bm), 2.94−3.15 (bm), 3.37 (bs), 3.54 (bs), 3.64 (bm), 3.76 (bs), 4.28−4.53 (bm), 5.21−5.49 (bm), 6.65−7.53 (bm). ^{13}C NMR ($CDCl_3$): δ 13.6, 32.4, 39.1−40.9 (m), 43.4, 50.2, 55.9, 59.3, 69.6−72.1 (m), 73.2, 85.5, 101.0, 112.6, 113.1, 115.4, 127.7−128.0 (m), 129.4, 131.1, 133.0, 133.8, 136.5, 137.6, 138.2, 139.6, 156.5, 168.4, 170.1. ^{1}H NMR and ^{13}C NMR spectra for the remaining copolymers have identical peak assignments with varying intensities for each block (see Table 1).

General Procedure for the Preparation of Nanoparticle Solutions. Aqueous solutions of the block copolymers listed in Table 1 were prepared by dialysis. Stock solutions of copolymers (0.1 wt %) in DMSO were stirred for 4 h at room temperature to ensure complete polymer solubilization. The stock solutions were diluted for the preparation of nanoparticles from 0.01 and 0.001 wt % copolymer. Ultrapure water (Millipore 18.2 MΩ cm resistivity) was added to the stirring copolymer solutions at a rate of 1 drop (10 μL, 0.35 wt %) per every 10 s using a micropipet until the solution contained 15 wt % water. The resulting aggregate solutions were placed in dialysis tubes (Spectra/Por RC, 3-mL Float-a-Lyzer, MWCO = 3500) and dialyzed against ultrapure water in 500-mL Erlenmeyer flasks with the dialysis solution changed every 2−3 h. Complete removal of DMSO from the filtrate after 48 h was verified by UV−vis spectroscopy as indicated by the disappearance of the UV cutoff for DMSO at 268 nm.

Transmission Electron Microscopy. Transmission electron microscopy (TEM) was performed on a Hitachi H8100 microscope operating at an accelerating voltage of 200 kV. For the observation of the size and distribution of the copolymer nanoparticles, samples (5 μL) were deposited from aqueous solutions of the copolymers, immediately after dialysis, onto copper EM grids (400 mesh, Formvar/carbon-coated). Water was allowed to evaporate from the grids at atmospheric pressure and room temperature. Negative staining was performed by exposing the grids to a solution of 2-wt % uranyl acetate (5 μL) for 2 min. The grids were tapped dry with filter paper to remove the excess stain. The samples were air-dried before TEM measurement. Average diameters (and standard deviations) were obtained directly from the negative TEM images over a sample of 100 particles.

Light-Scattering Measurements. Dynamic light-scattering (DLS) measurements were performed on a Brookhaven Instruments Corp. photon correlation spectrometer (BI-200 SM goniometer) fitted with a Brookhaven Instruments BI-9000AT digital correlator and a 300-mW argon ion laser at 514 nm. The scattering angle used was 90°. A refractive index-matching bath of filtered decalin (0.2 μm) surrounded the scattering cell, and the temperature was fixed at 25 °C. Correlation data were fitted, using the method of cumulants,[22] to the logarithm of the correlation function, yielding the diffusion coefficient, *D*. The hydrodynamic diameters (*d*) of the nanoparticles were calculated using *D* and the Stokes−Einstein equation ($D = k_BT/3\pi\eta d$, where k_B is the Boltzmann constant, *T* is the absolute temperature, η is the solvent viscosity, and *d* is the diameter of the particle). The polydispersity factor of the nanoparticles, represented as μ_2/Γ^2, where μ_2 is the second cumulant of the decay function and Γ is the average characteristic line width, was calculated by the cumulant method. CONTIN algorithms[23] were used in the Laplace inversion of the autocorrelation functions to confirm particle size distributions. All analyses were performed with the supplied instrument software.

Static light-scattering experiments were performed on a DAWN-EOS multi-angle laser photometer (Wyatt Technology, Santa Barbara, CA) equipped with a He−Ne laser (632.8 nm). Measurements were recorded in batch mode at room temperature, and the copolymer solutions were prepared by dissolving the copolymers in DMSO. Different concentrations were obtained by stepwise dilution of the concentrated samples. The solutions were filtered through membrane filters (0.45 μm). Ultrapure water (Millipore 18.2 MΩ cm resistivity) was added to the copolymer/DMSO solutions with a micropipet. The scattered light intensity was recorded 5 min after the addition of water and stirring of the solution.

In Vitro Indomethacin Release Experiments. Nanoparticle solutions (3.0 mL, 15 wt % H_2O in DMSO) containing 0.1 wt % of the copolymer were prepared as stated above. The solutions were transferred to prewashed dialysis tubes (Spectra/Por RC, 3-mL Float-a-Lyzer, MWCO = 3500) and incubated in an HCl-buffered DMSO/H_2O (4:1, v/v) mixture (pH = 3.0) (42 mL) with rapid stirring in a temperature-controlled oil bath at (a) 25 °C and (b) 37 °C. The release of indomethacin was monitored after 48 h by measuring the absorbance at 320 nm of the solution in the outer chamber.

Results and Discussion

Monomer Synthesis. Norbornene-based monomers incorporating indomethacin, a nonsteroidal antiinflammatory[24] and antitumor agent[25] (**4**, Scheme 1A), and hexaethylene glycol monomethyl ether (**5**, Scheme 1B) were selected as pendant hydrophobic and hydrophilic moieties, respectively, for the generation of amphiphilic drug-containing block copolymers. Both compounds were synthesized from α-bromo-α′-(*exo*-5-norbornene-2-ol)-*p*-xylene (**1**).[20] Treatment of **1** with potassium phthalimide in DMF resulted in the phthalimide adduct **2** which was then treated with hydrazine to yield the amine derivative **3**, all in high yields. Condensation of **3** with *N*-hydroxysuccinimide-activated indomethacin[21] gave the amide-linked norbornenyl-modified indomethacin **4**. The water-soluble monomer **5** was obtained in one

Scheme 1. Synthesis of Monomers 4 and 5[a]

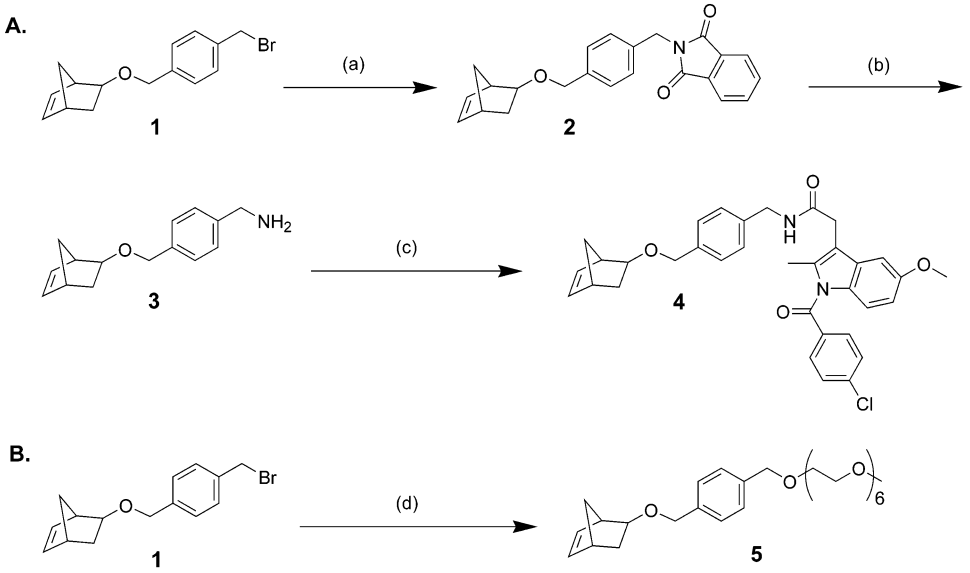

[a] (a) Potassium phthalimide, DMF, 92%; (b) H_2NNH_2, EtOH, 95%; (c) indomethacin−NHS,[21] DMF, 93%; (d) PEG−ONa, THF, 96%.

Scheme 2. Synthesis of Amphiphilic Block Copolymers 4_m-*b*-5_n

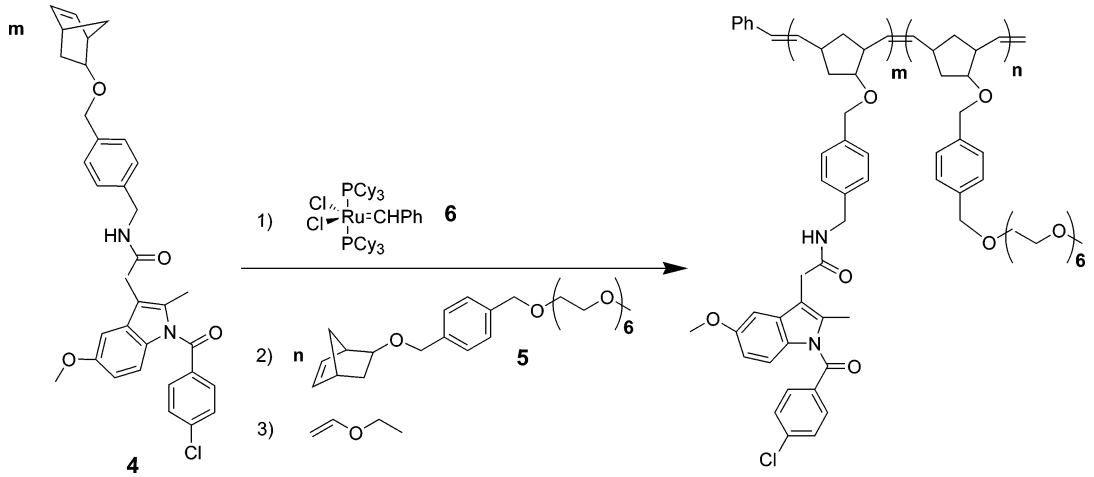

step by treatment of **1** with the sodium salt of hexaethylene glycol monomethyl ether.

Polymerization Studies. To test the ROMP activity of **4** and **5** with $Cl_2(PCy_3)_2Ru{=}CHPh$ (Grubbs catalyst) (**6**), NMR-scale polymerization experiments were monitored by ^1H NMR spectroscopy. As expected, both **4** and **5** were susceptible to ROMP as evidenced by the loss of resonances associated with the olefinic protons of the norbornene unit in each monomer (at 5.9 and 6.2 ppm, respectively) after 20 min and the simultaneous growth of broad olefinic resonances associated with the resulting polymers (from 5.2 to 5.5 ppm).

Upon verification of the polymerization reactivity of **4** and **5**, larger scale polymerization experiments were carried out at the same concentration as that of the NMR-scale experiments to yield a series of amphiphilic block copolymers (Scheme 2). Control over copolymer chain length and block composition was demonstrated by varying monomer/catalyst ($[M]_0/[C]_0$) ratios. In each experiment, monomer **4** was treated with catalyst **6** and polymerized to completion, at which time the desired equivalents of monomer **5** were added and allowed to stir until all monomer was consumed. The reactions were quenched by the addition of ethyl vinyl ether,[26] and the resulting AB block copolymers (denoted $\mathbf{4}_m$-*b*-$\mathbf{5}_n$, where *m* and *n* are the number of repeat units of the **4** and **5** blocks, respectively) were isolated by precipitation from hexanes. In all cases, quantitative yields of copolymer were obtained. The resulting copolymers (entries 1−6, Table 1) were characterized by GPC, ^1H NMR, and ^{13}C NMR.

Figure 1 shows the stepwise block polymerization profile monitored by GPC for copolymer $\mathbf{4}_{35}$-*b*-$\mathbf{5}_{35}$, as a representative example. After polymerization of **4** is initiated with **6**, the number-average molecular weight (M_n) and polydispersity index (PDI = M_w/M_n) were

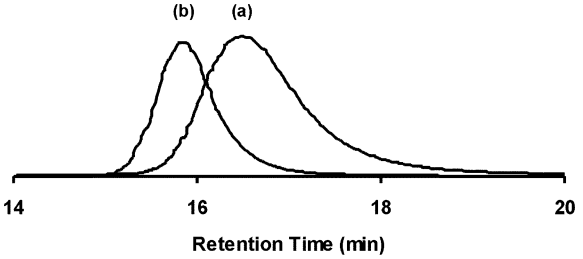

Figure 1. Gel-permeation chromatograms of (a) block $\mathbf{4}_{35}$ and (b) final diblock copolymer $\mathbf{4}_{35}$-*b*-$\mathbf{5}_{35}$.

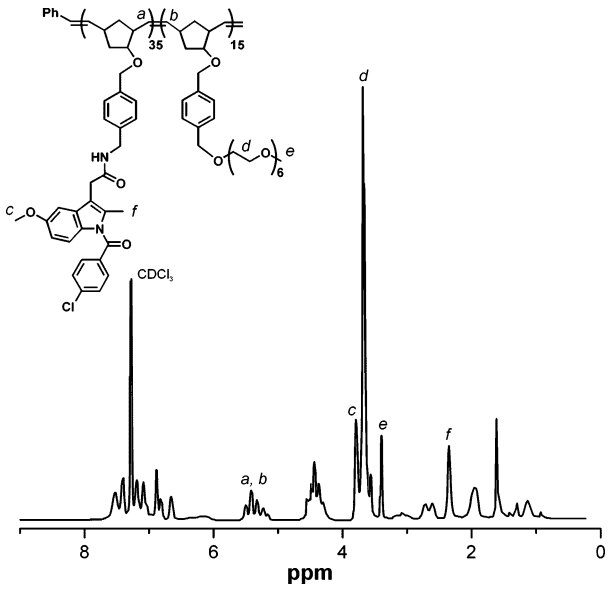

Figure 2. The ^{1}H NMR spectrum of block copolymer $\mathbf{4}_{35}$-*b*-$\mathbf{5}_{15}$ in $CDCl_3$.

17 100 and 1.21, respectively. The M_n of the block containing monomer **4** is consistent with the initial $[M]_0/[C]_0$ ratio. Upon block copolymerization of monomer **5**, the M_n increases to 35 100 without broadening of the molecular weight distribution (PDI = 1.08), which is in accordance with the $[M]_0/[C]_0$ ratio. Similar results were obtained for all of the block copolymers investigated in this study.

The ^{1}H NMR spectra of the block copolymers also provide information on copolymer composition. As a representative example, the ^{1}H NMR spectrum for $\mathbf{4}_{35}$-*b*-$\mathbf{5}_{15}$ is shown in Figure 2. Besides the major resonances arising from the polymer backbone and the benzyl ether spacing groups for each block, distinct signals assignable to the indomethacin moiety in **4** (*c*, *f*) and the ethylene oxide and terminal methoxy units in **5** (*d*, *e*) are observed. A trans-to-cis ratio of 2.4/1 was determined by integrating the peaks of the corresponding olefinic protons (*a*, *b*) of the polynorbornene backbone. The other copolymers investigated had trans-to-cis ratios ranging from 2.8/1 to 2.0/1 (Table 1). On the basis of relative peak integration between the methyl protons from monomer **4** (*f*) and the methoxy protons from monomer **5** (*e*), the ratio of **4** to **5** in the copolymer chain was estimated to be 2.6/1, which is consistent with the reaction stoichiometry of 2.3/1. The ratios of repeating unit **4** to repeating unit **5** for the other copolymers, listed in Table 1, are each consistent with the respective reaction stoichiometry.

Aggregation of Block Copolymers. To develop a nanoparticle system with potential therapeutic applications, it is necessary to exhibit control over the size and morphology of the polymeric aggregates. In a previous study, Yaun et al. reported the size cutoff for tumor vascular permeability of macromolecular aggregates to be approximately 400 nm[27] with the ideal size to be about 100 nm. Thus, we sought to reliably control the aggregation morphology and size distribution of our drug-containing copolymers to meet this criterion. The impact of copolymer chain length, the molar composition ratio of repeating units of block **4** to **5**, and the initial copolymer loading in DMSO on the aggregation morphology and size distribution of the nanoparticles were investigated.

Table 2. Properties of Polymeric Nanoparticles

entry	copolymer	wt %[a]	d[b] (TEM), nm	d (DLS), nm	μ_2/Γ^2 [c]	cwc (wt %)
1	$\mathbf{4}_{89}$-*b*-$\mathbf{5}_{11}$	0.1	993 ± 270	1600	0.13	
2	$\mathbf{4}_{75}$-*b*-$\mathbf{5}_{25}$	0.1	755 ± 420	780	0.22	
3	$\mathbf{4}_{50}$-*b*-$\mathbf{5}_{50}$	0.1	830 ± 420	1000	0.26	
4	$\mathbf{4}_{35}$-*b*-$\mathbf{5}_{35}$	0.1	504 ± 120	600	0.20	3.15
5	$\mathbf{4}_{35}$-*b*-$\mathbf{5}_{15}$	0.1	407 ± 47	480	0.08	2.90
6	$\mathbf{4}_{35}$-*b*-$\mathbf{5}_{7}$	0.1	390 ± 50	450	0.22	2.80
7	$\mathbf{4}_{35}$-*b*-$\mathbf{5}_{7}$	0.01	168 ± 20	180	0.05	3.50
8	$\mathbf{4}_{35}$-*b*-$\mathbf{5}_{7}$	0.001	94 ± 14	130	0.07	4.61

[a] Initial copolymer loading in DMSO prior to water addition. [b] Number-average diameter and standard deviation by TEM. [d] Polydispersity factor (see Experimental Section).

The copolymer samples listed in Table 1 were not directly soluble in water, even at elevated temperature, presumably due to the large weight fraction of the hydrophobic blocks and the inherent hydrophobicity of the aliphatic backbones in each sample. Hence, it was impossible to prepare polymeric aggregates from them via direct dissolution in water. An alternate strategy, developed by Eisenberg and co-workers for the preparation of "crew-cut" micelles,[28,29] was adopted to induce aggregation of our amphiphilic block copolymers. To form stable aggregates in an aqueous environment, it was necessary to first dissolve the copolymers in DMSO, which is a common solvent for both blocks. Subsequently, ultrapure water (Millipore, 18.2 MΩ cm resistivity) was added to each stirring copolymer solution at room temperature to induce aggregation of the blocks containing the hydrophobic monomer **4**. Copolymer aggregation, as indicated by static light-scattering experiments, typically occurred at ca. 3−5 wt % water addition depending on copolymer composition. The water content was gradually increased at the same rate until the solutions contained 15 wt % water. The resulting solutions were then dialyzed against ultrapure water. DMSO can be completely removed from the solution after 24−48 h, as verified by UV−vis spectroscopy. After dialysis, aliquots of each of the aqueous aggregate solutions were redissolved in DMSO, and the copolymer concentrations were determined from UV−vis spectroscopy. Complete mass conservation of copolymer after dialysis was found for all samples. The resulting polymeric aggregates were characterized by TEM, DLS, and ^{1}H NMR.

The transmission electron micrographs of a representative selection of the copolymer nanoparticles are shown in Figure 3. All of the copolymers assembled in aqueous media to form spherical particles with varying size distributions. Mean hydrodynamic diameters (d) and the corresponding polydispersity factors (μ_2/Γ^2) were determined by DLS measurements performed at 90°. Upon confirming the spherical nature of the aggregates by TEM, the angular dependence of the average characteristic line widths (Γ/K^2) was assumed to be negligible.

The aggregates prepared from the copolymers with chain lengths of 100 repeat units were rather large. The mean diameters (d) of the particles obtained from copolymers $\mathbf{4}_{89}$-*b*-$\mathbf{5}_{11}$, $\mathbf{4}_{75}$-*b*-$\mathbf{5}_{25}$, and $\mathbf{4}_{50}$-*b*-$\mathbf{5}_{50}$, measured by DLS, were 1600, 780, and 1000 nm, respectively (entries 1−3, Table 2). The corresponding polydispersity factors (μ_2/Γ^2), estimated by the cumulant method, of 0.13, 0.22, and 0.26, respectively, suggested broad size distributions that were further confirmed by CONTIN analysis. The spherical shape and broad size distribu-

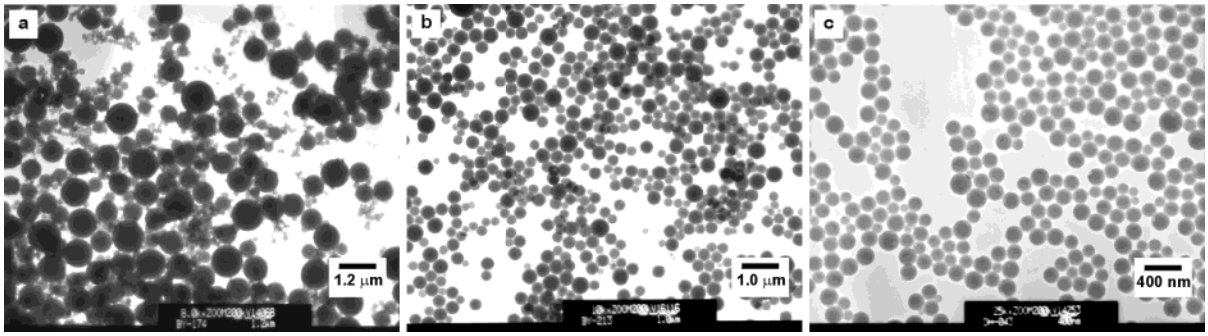

Figure 3. TEM images of nanoparticles from copolymers (a) $\mathbf{4}_{89}$-*b*-$\mathbf{5}_{11}$ (entry 1, Table 2), (b) $\mathbf{4}_{35}$-*b*-$\mathbf{5}_{15}$ (entry 5, Table 2), and (c) $\mathbf{4}_{35}$-*b*-$\mathbf{5}_{7}$ (entry 7, Table 2).

tion of these polymeric aggregates were also confirmed by TEM (Figure 3a, for $\mathbf{4}_{89}$-*b*-$\mathbf{5}_{11}$). The particle diameters and size distributions calculated by TEM are in agreement with the DLS results. The larger diameters obtained by light scattering may be attributed to a swelling of the shell-forming blocks in aqueous solution. That the sizes of the aggregates are larger than would be expected, based on the average copolymer chain length, for copolymer micelles suggests the existence of multicore-type micellar structures[30,31] or colloidal micelle-like aggregates of insoluble copolymer self-stabilized by hydrophilic **5** blocks on the surface (vide infra). Previous reports have indicated that amphiphillic block copolymers with short poly(ethylene oxide) (PEO) blocks frequently form large aggregates in aqueous solution.[32,33]

Reducing the overall copolymer chain length significantly decreased the mean diameters of the resulting nanoparticles (cf. entries 3 and 4, Table 2). In addition, maintaining a constant block length of monomer **4** while reducing the block length of monomer **5** resulted in a regular decrease in mean diameter from 600 to 450 nm (entries 4−6, Table 2). Again, a good agreement exists between the average diameters obtained by microscopy and light scattering. Interestingly, for copolymer $\mathbf{4}_{35}$-*b*-$\mathbf{5}_{15}$, the DLS polydispersity factor of the 0.1-wt % nanoparticles is 0.08, indicating a very narrow size distribution.[34] The preserved spherical aggregation morphology and uniform size distribution of the aggregates from copolymer $\mathbf{4}_{35}$-*b*-$\mathbf{5}_{15}$ were again confirmed by TEM (Figure 3b).

The initial copolymer loading in DMSO prior to water addition also affected the size and distribution of the nanoparticles as illustrated for copolymer $\mathbf{4}_{35}$-*b*-$\mathbf{5}_{7}$ (entries 6−8, Table 2). Decreasing the copolymer loading from 0.1 to 0.001 wt % resulted in a steady decrease in mean hydrodynamic diameter from 450 to 130 nm accompanied by a narrowing of the size distributions as determined by DLS. The corresponding average diameters obtained by TEM also decreased from 390 to 94 nm (entries 6−8, Table 2). Figure 3c displays a representative TEM image of the nanoparticles formed from a 0.01 wt % solution of copolymer $\mathbf{4}_{35}$-*b*-$\mathbf{5}_{7}$ (entry 7, Table 2). Dilution of the copolymer aggregate solutions obtained after dialysis had no effect on the diameters and size distributions of the nanoparticles as measured by DLS, indicating that the aggregates are quite stable with respect to Ostwald ripening. Further, a continuous monitoring of copolymer aggregation by TEM during the water addition process suggests that the composition of each nanoparticle is set upon 3−5 wt % water addition (vide infra).

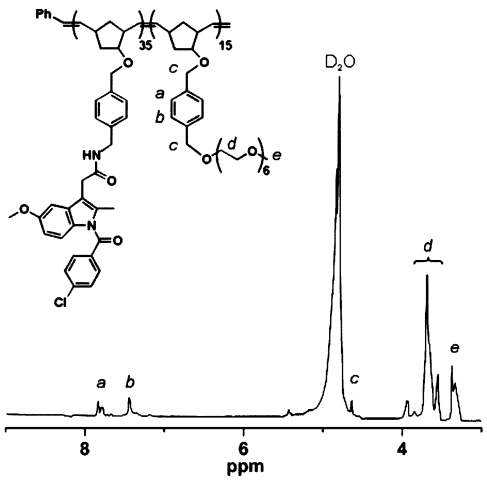

Figure 4. The ^{1}H NMR spectrum of block copolymer $\mathbf{4}_{35}$-*b*-$\mathbf{5}_{15}$ in D_2O after micellization (entry 5, Table 2).

To verify the envisaged core−shell structure of the copolymeric nanoparticles, sample solutions of the nanoparticles were lyophilized and redispersed in D_2O. ^{1}H NMR studies were then conducted on the D_2O dispersion with solvent suppression. Figure 4 shows the spectrum obtained from a D_2O-redispersed solution of the nanoparticles made from copolymer $\mathbf{4}_{35}$-*b*-$\mathbf{5}_{15}$ (entry 5, Table 2). As compared to the ^{1}H NMR spectrum of the same lyophilized materials redissolved in $CDCl_3$ (exact same spectrum as that shown in Figure 2), resonances associated with the indomethacin moiety in monomer **4** are suppressed, indicating that the protons associated with the block **4** segments are in solid, glassy environment.[35] In contrast, protons associated with the monomer **5** blocks could be clearly assigned. Peaks corresponding to the ethylene oxide units were observed at 3.64 ppm (*d*) as were those associated with the terminal methoxy group at 3.37 ppm (*e*). From the benzyl ether spacing group, the peak at 4.63 ppm was assigned to the methylene protons and the peaks at 7.45 and 7.84 ppm to the aromatic protons. Hence, for these systems, monomer **5** blocks must be in a solvated state. From these observations, it was concluded that our copolymer nanospheres existed as core−shell type structures composed of hydrophobic **4** blocks in a glassy state stabilized by outer shells of hydrophilic **5** blocks in water.

To gain a further understanding of the effects of copolymer concentration and composition on the aggregation process, critical water content (cwc) values of copolymers $\mathbf{4}_{35}$-*b*-$\mathbf{5}_{35}$, $\mathbf{4}_{35}$-*b*-$\mathbf{5}_{15}$, and $\mathbf{4}_{35}$-*b*-$\mathbf{5}_{7}$ in DMSO were determined by static light-scattering (Table 2). The cwc of a copolymer solution, defined as the water content

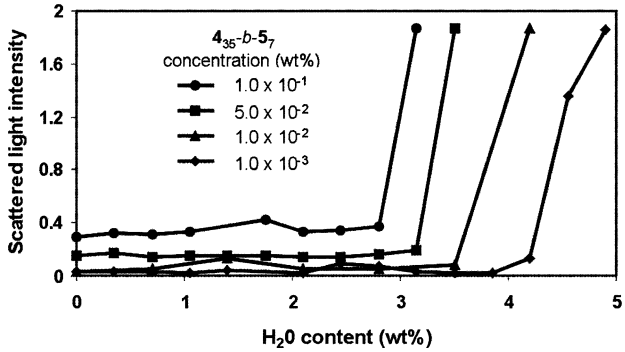

Figure 5. Scattered light intensity as a function of added water content for different concentrations of copolymer $\mathbf{4}_{35}$-*b*-$\mathbf{5}_7$ in DMSO.

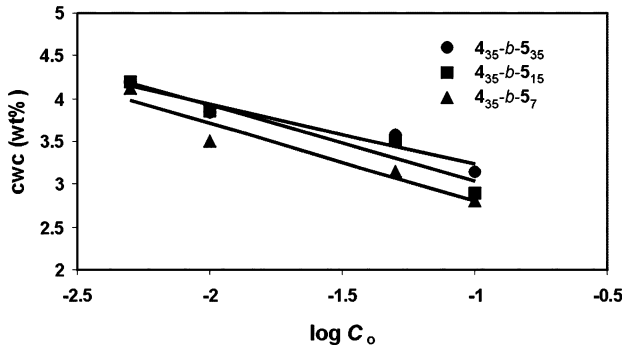

Figure 6. Critical water content versus logarithm of copolymer concentration in DMSO for $\mathbf{4}_{35}$-*b*-$\mathbf{5}_7$, $\mathbf{4}_{35}$-*b*-$\mathbf{5}_{15}$, and $\mathbf{4}_{35}$-*b*-$\mathbf{5}_{35}$.

at which copolymer aggregation begins, is obtained from the intercept of the horizontal and vertical line segments of the static light-scattering curve.[36] Below a critical value, the water content in a copolymer solution has relatively little effect on the scattered light intensity, implying that the dimensions of the copolymer chains do not change appreciably. However, upon reaching the cwc, the scattered light intensity increases significantly, indicating the onset of phase separation and aggregation. As a representative example, a plot of the scattered light intensity as a function of copolymer concentration for $\mathbf{4}_{35}$-*b*-$\mathbf{5}_7$ is given in Figure 5. The cwc shifts to higher water contents as the initial copolymer concentration in DMSO decreases (entries 6−8, Table 2). A similar trend was observed for copolymers $\mathbf{4}_{35}$-*b*-$\mathbf{5}_{15}$ and $\mathbf{4}_{35}$-*b*-$\mathbf{5}_{35}$.

Figure 6 shows the cwc values as a function of copolymer concentration for $\mathbf{4}_{35}$-*b*-$\mathbf{5}_{35}$, $\mathbf{4}_{35}$-*b*-$\mathbf{5}_{15}$, and $\mathbf{4}_{35}$-*b*-$\mathbf{5}_7$. A linear relationship is found between the cwc for each copolymer and the base-10 logarithm of the copolymer concentration. It is interesting to note that, for a specific concentration of copolymers, the cwc increases as the molecular weight of the copolymer increases (entries 4−6, Table 2). This indicates that, for a fixed hydrophobic block length, increasing the length of the hydrophilic block (from $\mathbf{4}_{35}$-*b*-$\mathbf{5}_7$ to $\mathbf{4}_{35}$-*b*-$\mathbf{5}_{35}$) allows the copolymers to remain soluble at higher water contents despite the increase in molecular weight.

It has been shown in a previous report—in which polystyrene-*b*-poly(acrylic acid) (PS-*b*-PAA) micelles were prepared by the addition of water to the respective copolymer solutions in *N*,*N*-dimethylformamide (DMF)—that at the cwc, the initial copolymer concentration, C_0, actually represents the critical micelle concentration (C_{cmc}, the concentration of the unassociated polymer chains).[36] As water is added to copolymer solutions beyond the cwc, more and more copolymer chains associate to form micelles, and the concentration of single-chain copolymers decreases. From this relationship, the micelle fraction, defined as the ratio of associated copolymer chain to the total number of chains, can be calculated using the following expression:[36]

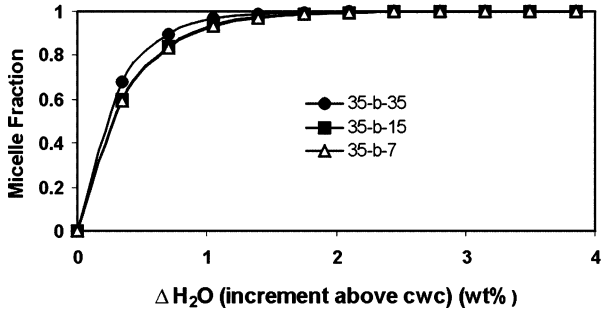

Figure 7. Micelle fraction as a function of water increment beyond the critical water content for copolymers $\mathbf{4}_{35}$-*b*-$\mathbf{5}_7$, $\mathbf{4}_{35}$-*b*-$\mathbf{5}_{15}$, and $\mathbf{4}_{35}$-*b*-$\mathbf{5}_{35}$.

$$(C_0 - C_{cmc})/C_0 = 1 - \exp(-2.303\Delta H_2O/A)$$

where C_0 represents the initial copolymer concentration, C_{cmc} represents the critical micelle concentration, ΔH_2O is the increment of the water content beyond the cwc, and A is obtained from the slope d[cwc]/d[log C_0] (Figure 6). If the water content in solution is below the cwc (ΔH_2O is zero or less), the micelle fraction is zero and all of the copolymer chains in solution are unassociated.

A plot of the micelle fraction as a function of the increment of water in solution above the cwc for copolymers $\mathbf{4}_{35}$-*b*-$\mathbf{5}_{35}$, $\mathbf{4}_{35}$-*b*-$\mathbf{5}_{15}$, and $\mathbf{4}_{35}$-*b*-$\mathbf{5}_7$ is shown in Figure 7. For each copolymer, the micelle fraction increases dramatically within a very narrow range of water contents after the onset of phase separation at the cwc. Indeed, complete micellization (>99.5%) is achieved at an increment of 1.75 wt % beyond the cwc for copolymer $\mathbf{4}_{35}$-*b*-$\mathbf{5}_{35}$ and 2.10 wt % for copolymers $\mathbf{4}_{35}$-*b*-$\mathbf{5}_{15}$ and $\mathbf{4}_{35}$-*b*-$\mathbf{5}_7$. These results confirm that copolymer aggregation is complete at water contents below 15 wt %, the point at which our copolymer solutions are subjected to dialysis and the indomethacin release experiments were carried out (see Experimental Section).

In Vitro Indomethacin Release. The release of indomethacin from $\mathbf{4}_{35}$-*b*-$\mathbf{5}_7$ nanoparticles upon exposure to acidic conditions was investigated via a dialysis experiment. The results are shown in Figure 8. Nanoparticles were prepared from a 0.1-wt % copolymer solution and incubated in a HCl-adjusted mixture of H_2O/DMSO (pH = 3.0, 20 wt % H_2O) in a dialysis tube located within a magnetically stirred dialysis chamber for 48 h. The amount of indomethacin released from the particles was determined by measuring the UV absorbance (at λ = 320 nm) of the outer chamber solution. The total weight of the copolymer and the percentage of indomethacin-susbtituted monomer was used to calculate the concentration of indomethacin at 100% release from the copolymer. As a control experiment, indomethacin (at the theoretical 100%-release concentration) was incubated at room temperature. After 48 h, the absorbance of the solution in the outer chamber of the dialysis setup matched the calculated value, indicating free diffusion of indomethacin through the membrane and complete equilibration of the solution.

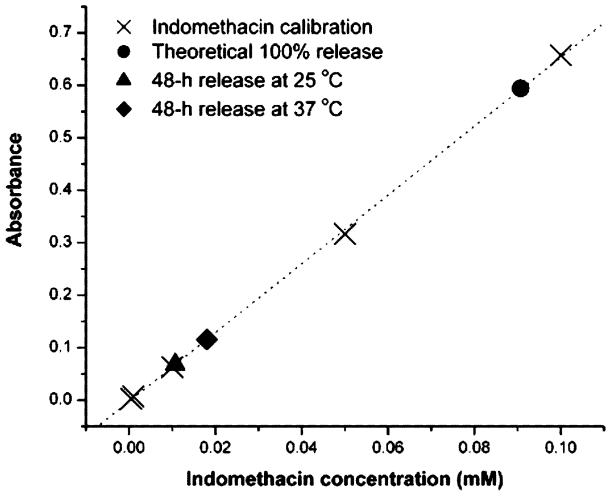

Figure 8. In vitro release of indomethacin from copolymer $\mathbf{4}_{35}$-*b*-$\mathbf{5}_7$ nanoparticles after 48 h in pH = 3.0 H_2O/DMSO (4:1, v/v) at (▲) 25 °C and (◆) 37 °C.

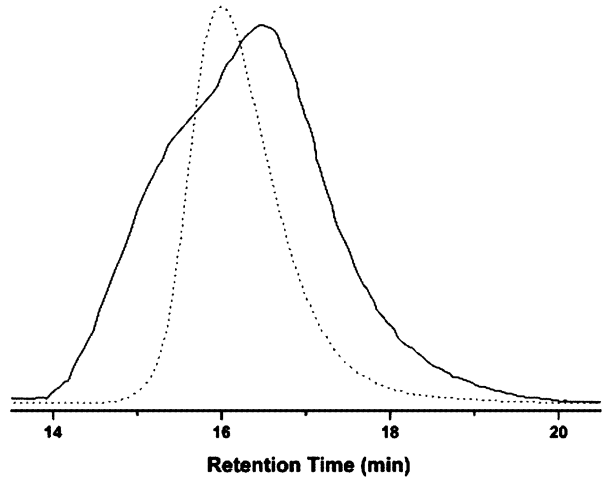

Figure 9. Gel-permeation chromatograms of copolymer $\mathbf{4}_{35}$-*b*-$\mathbf{5}_7$ before (···) (PDI = 1.16) and after (−) (PDI = 1.67) incubation at 37 °C for 48 h in acidic media (pH = 3).

For nanoparticles prepared from copolymer $\mathbf{4}_{35}$-*b*-$\mathbf{5}_7$, 12% of the indomethacin was released after 48 h at 25 °C. Increasing the temperature of the surrounding medium to 37 °C resulted in 20% release after 48 h. The copolymer solutions were removed from the dialysis tubes after 48 h and characterized by GPC. As shown in Figure 9, degradation of the copolymer has occurred consistent with the release of indomethacin. These results are comparable to those reported for the release of physically entrapped indomethacin from block-copolymer nanospheres composed of poly(ethylene glycol)/DL-lactide[37] and poly(ethylene glycol)/ϵ-caprolactone,[38] suggesting that the release of our covalently linked indomethacin is actually quite facile.

In summary, we have demonstrated that well-defined amphiphilic block copolymers composed of indomethacin and hexa(ethylene oxide) norbornene-based monomers may be used to form core−shell polymeric nanoparticles in aqueous media. Average particle diameters were in the range of 90−1000 nm (TEM) and 130−1600 nm (DLS), the smallest values obtained from the shortest copolymers in the most dilute solutions. For nanoparticles prepared from copolymer $\mathbf{4}_{35}$-*b*-$\mathbf{5}_7$, 20% of the indomethacin was released after 48 h at 37 °C in an acidic environment. Significantly, our work represents a unique example of the construction of ROMP-based drug-containing polymeric nanoparticles with a high-density of drugs that exhibit well-defined morphologies and size distributions relevant to therapeutic applications. Although we only illustrate the formation of nanoparticles from diblock copolymers in this work, the incorporation of a multiblock copolymer containing several drugs in the hydrophobic segment is possible[18] and should be applicable to multi-agent chemotherapeutic regimes. The ability to design and synthesize complex architectures from readily available easily modified polymer subunits from ROMP makes this approach accessible and facile. The generality of this unique approach to the assembly of drug-containing polymeric nanoparticles from functionalized copolymers is currently under investigation.

Acknowledgment. Financial support by the NU Institute for Bioengineering and Nanoscience in Advanced Medicine (IBNAM), Baxter Healthcare, Inc., Robert H. Lurie Comprehensive Cancer Center, AFOSR (PECASE Grant F49620-01-1-0303), and NSF (DMR-CAREER Grant 0094347) is appreciated. S.T.N. is an Alfred P. Sloan research fellow. We acknowledge the use of instruments in the Keck Biophysics Facility and Electron Probe Instrumentation Center at Northwestern University.

References and Notes

(1) Choucair, A.; Eisenberg, A. *Eur. Phys. J. E* **2003**, *10*, 37−44.
(2) Tuzar, Z. *NATO ASI Ser., Ser. E* **1996**, 327, 309−318.
(3) Riess, G.; Dumas, P.; Hurtrez, G. *Microspheres, Microcapsules & Liposomes* **2002**, *5*, 69−110.
(4) Moffitt, M.; Khougaz, K.; Eisenberg, A. *Acc. Chem. Res.* **1996**, *29*, 95−102.
(5) Allen, C.; Eisenberg, A.; Maysinger, D. *S.T.P. Pharma Sci.* **1999**, *9*, 139−151.
(6) Kataoka, K.; Harada, A.; Nagasaki, Y. *Adv. Drug Delivery Rev.* **2001**, *47*, 113−131.
(7) Kabanov, A. V.; Alakhov, V. Y. In *Amphiphilic Block Copolymers: Self-Assembly and Applications*; Alexandridis, P., Lindman, B., Eds.; Elsevier: Netherlands, 1997; p 435.
(8) Singla, A. K.; Garg, A.; Aggarwal, D. *Int. J. Pharm.* **2002**, *235*, 179−192.
(9) Pratten, M. K.; Lloyd, J. B.; Hoerpel, G.; Ringsdorf, H. *Makromol. Chem.* **1985**, *186*, 725−733.
(10) Kataoka, K.; Matsumoto, T.; Yokoyama, M.; Okano, T.; Sakurai, Y.; Fukushima, S.; Okamoto, K.; Kwon, G. S. *J. Controlled Release* **2000**, *64*, 143−153.
(11) Yokoyama, M.; Fukushima, S.; Uehara, R.; Okamoto, K.; Kataoka, K.; Sakurai, Y.; Okano, T. *J. Controlled Release* **1998**, *50*, 79−92.
(12) Yoo, H. S.; Park, T. G. *J. Controlled Release* **2001**, *70*, 63−70.
(13) Matsumura, Y.; Maeda, H. *Cancer Res.* **1986**, *46*, 6387−6392.
(14) Halaban, R.; Patton, R. S.; Cheng, E.; Svedine, S.; Trombetta, E. S.; Wahl, M. L.; Ariyan, S.; Hebert, D. N. *J. Biol. Chem.* **2002**, *277*, 14821−14828.
(15) Lynn, D. M.; Mohr, B.; Grubbs, R. H. *J. Am. Chem. Soc.* **1998**, *120*, 1627−1628.
(16) Schwab, P.; France, M. B.; Grubbs, R. H.; Ziller, J. W. *Angew. Chem., Int. Ed. Engl.* **1995**, *34*, 2039−2041.
(17) Kiessling, L. L.; Strong, L. E. *Top. Organomet. Chem.* **1998**, *1*, 199−231.
(18) Watson, K. J.; Anderson, D. R.; Nguyen, S. T. *Macromolecules* **2001**, *34*, 3507−3509.
(19) The incorporations of PEG segments to polymeric drugs have been shown to prevent protein binding and suppress immunological reactions by the reticular endothelial system, thereby providing biocompatibility in drug delivery applications. See: Maeda, H.; Seymour, L. W.; Miyamoto, Y. *Bioconjugate Chem.* **1992**, *3*, 351−362.
(20) Watson, K. J.; Nguyen, S. T.; Mirkin, C. A. *J. Organomet. Chem.* **2000**, *606*, 79−83.
(21) Singh, P.; Hingorani, L. L.; Trivedi, G. K. *Indian J. Chem., Sect. B* **1990**, *29B*, 551−555.

(22) Koppel, D. E. *J. Chem. Phys.* **1972**, *57*, 4814−4820.
(23) Provencher, S. W. *Makromol. Chem.* **1979**, *180*, 201−209.
(24) Fawaz, F.; Bonini, F.; Guyot, M.; Lagueny, A. M.; Fessi, H.; Devissaguet, J. P. *Int. J. Pharm.* **1996**, *133*, 107−115.
(25) Golab, J.; Kozar, K.; Kaminski, R.; Czajka, A.; Marczak, M.; Switaj, T.; Giermasz, A.; Stoklosa, T.; Lasek, W.; Zagozdzon, R.; Mucha, K.; Jakobisiak, M. *Life Sci.* **2000**, *66*, 1223−1230.
(26) Wu, Z.; Nguyen, S. T.; Grubbs, R. H.; Ziller, J. W. *J. Am. Chem. Soc.* **1995**, *117*, 5503−5511.
(27) Yuan, F.; Dellian, M.; Fukumura, D.; Leunig, M.; Berk, D. A.; Torchilin, V. P.; Jain, R. K. *Cancer Res.* **1995**, *55*, 3752−3756.
(28) Li, Z.; Zhao, W.; Liu, Y.; Rafailovich, M. H.; Sokolov, J.; Khougaz, K.; Eisenberg, A.; Lennox, R. B.; Krausch, G. *J. Am. Chem. Soc.* **1996**, *118*, 10892−10893.
(29) Gao, Z.; Varshney, S. K.; Wong, S.; Eisenberg, A. *Macromolecules* **1994**, *27*, 7923−7927.
(30) Zhang, L.; Eisenberg, A. *Science* **1995**, *268*, 1728−1731.
(31) Zhang, L.; Eisenberg, A. *J. Am. Chem. Soc.* **1996**, *118*, 3168−3181.
(32) Xu, R.; Winnik, M. A.; Hallett, F. R.; Riess, G.; Croucher, M. D. *Macromolecules* **1991**, *24*, 87−93.
(33) Allen, C.; Yu, Y.; Maysinger, D.; Eisenberg, A. *Bioconjugate Chem.* **1998**, *9*, 564−572.
(34) Cao, T.; Yin, W.; Webber, S. E. *Macromolecules* **1994**, *27*, 7459−7464.
(35) Kim, S. Y.; Shin, I. G.; Lee, Y. M. *Biomaterials* **1999**, *20*, 1033−1042.
(36) Zhang, L.; Shen, H.; Eisenberg, A. *Macromolecules* **1997**, *30*, 1001−1011.
(37) Kim, S. Y.; Shin, I. G.; Lee, Y. M. *J. Controlled Release* **1998**, *56*, 197−208.
(38) Kim, S. Y.; Shin, I. G.; Lee, Y. M.; Cho, C. S.; Sung, Y. K. *J. Controlled Release* **1998**, *51*, 13−22.

MA035741+